

TOPOGRAPHIC CORRECTION FOR DIFFERENTIAL ILLUMINATION EFFECTS ON IKONOS SATELLITE IMAGERY

K.H. Law^a, J. Nichol^b

Department of Land Surveying and Geo-Informatics,
The Hong Kong Polytechnic University,
Hungghom, Kowloon, Hong Kong

^a samuel.law@polyu.edu.hk, ^b jsjanet@polyu.edu.hk

KEY WORDS: Remote Sensing, IKONOS, Algorithm, Correction, Test

ABSTRACT:

The problem of differential terrain illumination on satellite imagery has been investigated for at least 20 years and has not been solved satisfactorily. Most past research has been conducted on Landsat imagery where the look angle is nadir. There is no research on topographic correction of IKONOS imagery, which has a higher spatial resolution.

The high spatial resolution of IKONOS imagery requires a more accurate digital elevation model (DEM) than is obtained using standard interpolators. This paper assesses some existing topographic correction methods and applies them to off-nadir multispectral IKONOS-2 imagery in the mountainous terrain of Lam Tsuen country park in Hong Kong. The IKONOS-2 image was orthorectified using PCI Ortho Engine achieving an accuracy of approximately 4m over the whole image. Slope and aspect parameters derived from the terrain model were applied in different topographic correction algorithms. This research makes a contribution to existing knowledge on the subject. It demonstrates existing algorithms for topographic correction of satellite image can be successfully adapted to IKONOS images.

1. INTRODUCTION

1.1 Background

The spatial resolution of satellite images has increased in recent years. However, many images are affected by the system itself and by the environment e.g. geometric distortion and shadow due to topography. In order to interpret the satellite images effectively, these effects need to be minimized.

This study examines the application of existing topographic algorithms on IKONOS satellite image. Most past research about topographic correction has been conducted on Landsat imagery, e.g. (Teillet *et al.*, 1982; Justice and Holben, 1979; Civco, 1989) As IKONOS satellite imagery has 4m spatial resolution, which is comparatively high to traditional satellite sensors such as SPOT and LANDSAT, the accuracy requirements of both geometric correction and digital elevation model (DEM) for topographic correction need to be higher than before.

1.2 Objective

The objective of this study is to compare three existing methods of topographic correction and see how successfully they can be applied to IKONOS imagery.

2. BASIS OF THE STUDY

2.1 Image Used & Study Area

The satellite image used in this study is a 4m multi-spectral IKONOS imagery taken on 7 Sept 2002, with solar azimuth: 128.7341 degrees and solar elevation: 65.16463 degrees.

Lam Tsuen Country Park is chosen to be the study area. The mountain is oriented northeast to southwest and is located at the northern part of New Territories, Hong Kong. It has a relative relief 566m over an area of 5km x 5km. Its land cover types are mainly forest, herbaceous, grass, bare soil and buildings.

2.2 Creation of Digital Elevation Model (DEM)

Digital contour maps of 1:5000 scale produced by the Land Information Centre (LIC) of Lands Department in Hong Kong were used as a source of height information. The height separation of the contours in the digital map is 10 meters. A DEM with a resolution of 2m x 2m was created.

From the DEM dataset, information about the slope, aspect and illumination according to the sun angle and elevation were generated for input to the topographic corrections algorithms.

2.3 Geometric Correction

The IKONOS image used in this study was geometrically corrected to the HK80 grid coordinate system, which is the same as the digital maps.

In order to acquire a higher accuracy of the geocoded image, three different geometric corrections method were performed and tested. They are 2-D polynomial method, rational function method and rigorous model method. It was found that the rigorous model method, proposed by Toutin, 2000, gave the best result on the geometric correction of the IKONOS image with a root mean square error approximately one pixel (4m).

3. TOPOGRAPHIC CORRECTIONS

In this study, three topographic correction methods were tested and compared. They are the Cosine Correction, Minnaert Correction and a Normalization Method.

3.1 Cosine Correction

In this method, the surface is assumed to have Lambertian behaviour, i.e. to be a perfect diffuse reflector, having the same amount of reflectance in all view directions. Thus, the Lambertian correction function attempts to correct only for differences in illumination caused by the orientation of the surface (Jones *et al.*, 1988).

For the Lambertian assumption, the most widely used correction is this cosine method using the equation (1), (2) and (3), proposed by Teillet *et al.* (1982),

$$\cos i = \cos E \cos Z + \sin E \sin Z \cos(A_0 - A_S) \quad (1)$$

$$Ln(\lambda) = L(\lambda) / \cos i \quad (2)$$

$$L_H = L_T \cos z / \cos i \quad (3)$$

where L = radiance
 Z = solar zenith angle
 L_H = radiance for horizontal surface
 L_T = radiance observed over the inclined terrain
 i = incidence angle with respect to surface normal
 E = slope inclination
 Z = solar zenith angle
 A_0 = solar azimuth
 A_S = surface aspect of the slope angle

Although the Lambertian assumption is simple and convenient for topographic correction, there is a recognised problem in the corrected images. Thus when correcting the topographic effect under a Lambertian surface assumption, images tended to be over-corrected, with slopes facing away from the sun appearing brighter than sun-facing slopes due to diffuse sunlight being relatively more influential on the shady slope (Jones *et al.*, 1988). Therefore, non-Lambertian topographic correction method has been developed.

3.2 Minnaert Correction

In 1980, Smith *et al.* introduced an empirical photometric function, the Minnaert constant, to test the Lambertian assumption for surfaces. The Minnaert function was developed in 1941, and has been used for photometric analysis of lunar surfaces (Justice and Holben, 1979).

In the study by Smith *et al.* (1980), the Minnaert constant, k , was derived by first linearizing the equation below:

$$L(\lambda, e) = Ln \cos^{k(\lambda)} i \cos^{k(\lambda)-1} e \quad (4)$$

where L =radiance
 λ =wavelength
 e =slope angle
 L_n = radiance when $i=0$
 k = Minnaert constant
 i = incidence angle

$$L \cos e = Ln \cos^k i \cos^k e \quad (5)$$

After linearization, equation (2) becomes:

$$\log(L \cos e) = \log Ln + k \log(\cos i \cos e) \quad (6)$$

Now, we can obtain the regression value of k using equation (3), from the linear form of $y=mx+c$

where $x = \log(\cos i \cos e)$
 $y = \log(L \cos e)$
 $c = \log Ln$

The value of the Minnaert constant lies between 0 and 1. It is used to describe the roughness of the surface. When the surface has Lambertian behaviour, the value of the Minnaert constant is 1. Otherwise, it is less than 1.

After the Minnaert constant, k , is determined, a backwards radiance correction transformation model can be developed.

$$Ln = L(\cos e) / (\cos^k i \cos^k e) \quad (7)$$

If we compare this method with the non-Lambertian cosine method mathematically, it can be seen that the Minnaert constant, k , is used to weaken the power of topographic correction. In other words, it is used to describe the roughness of the surface of the terrain. As a result, the problem of over-correction in the area facing away from the sun can be solved.

3.3 Normalization Method

The normalization method used here is modified from the two-stage normalization proposed by Civco, 1989, and consists of two stages. In the first stage, shaded relief models, corresponding to the solar illumination conditions at the time of the satellite image are computed using the DEM data. This requires the input of the solar azimuth and altitude provided by the metadata of the satellite image. The resulting shaded relief model would have values between 0 and 255.

After the model is created, a transformation of each of the original bands of the satellite image is performed to derive topographically normalized images using equation (8).

$$\delta DN_{\lambda ij} = DN_{\lambda ij} + \left(\left(DN_{\lambda ij} \times \frac{(\mu_k - X_{ij})}{\mu_k} \right) \times C_{\lambda} \right) \quad (8)$$

where $\delta DN_{\lambda ij}$ = the normalized radiance data for pixel(i,j) in band(λ)
 $DN_{\lambda ij}$ = the raw radiance data for pixel(i,j) in band(λ)
 μ_k = the mean value for the entire scaled shaded relief model (0,255)
 X_{ij} = the scaled (0,255) illumination value for pixel(i,j)
 C_λ = the correction coefficient for band(λ)

In order to calculate the calibration coefficient, the spectral responses from large samples falling on the slope facing to and away from the sun need to be taken. The correction coefficient can be calculated using equation (9).

$$C_\lambda = \frac{(S_\lambda - N_\lambda)}{\left[\left(N_\lambda \times \frac{\mu_N - \mu_k}{\mu_k} \right) - \left(S_\lambda \times \frac{\mu_S - \mu_k}{\mu_k} \right) \right]} \quad (9)$$

where N_λ = the mean on the slope facing away the sun in the uncalibrated data for the forest category
 S_λ = the mean on the slope facing to the sun in the uncalibrated data for the forest category
 μ_k = the mean value for the entire scaled shaded relief model (0,255)
 μ_N = the mean of the illumination of forest on the slope facing away from the sun.
 μ_S = the mean of the illumination of forest on the slope facing to the sun.

As the main cover type on the shady slope is Forest, it is chosen to demonstrate calculation of the calibration coefficient. However, the calibration coefficient calculated will then perform best in this cover type.

4. RESULT AND DISCUSSION

4.1 Visual Analysis

As the visual effect is more impressive in the near-infrared band than in a visible band, a visual comparison of the false colour images is carried out. Figure 1 presents the false colour IKONOS images of, respectively, (a) the original, (b) cosine corrected, (c) Minnaert Corrected and (d) normalized images.

By comparing the images visually, we can see that figure 1(b) has the problem of overcorrection. The corrected image appears to be too bright in both the sun facing and sun-shaded slopes. From figure 1(c), the Minnaert corrected image, it is found that the visual effect on the slope facing away from the sun has improved significantly. Both the slope facing to the sun and slope facing away from the sun with same cover type appear to have similar brightness. However, it should be noted that the problem of cast-shadow, where the incident angle $i > 90$ degrees, is not handled in this correction method and remains to be uncorrected. From figure 1(d), it can be seen that there is

less improvement of brightness compared to figure 1(c). However, the increase in brightness of the slope facing away from the sun can still be seen.

4.2 Statistical Analysis

In order to test the accuracy of the topographic corrections statistically, training areas of forest and herbaceous covers were created on both sunny and shady slopes of the images. Mean values and standard deviations of the training areas for each band before and after the corrections were calculated and compared. Tables 1, 2, 3 show the mean values and standard deviations of the entire study area, herbaceous cover area and forest cover area respectively. If the correction is successful, the mean values of each cover types on the shady side should increase while those on the sunny side should decrease. For the values of standard deviations, if the correction is successful, the value of each class should decrease. Table 4 shows the DN mean value of different cover types on sunny slope and shady slope of band 4 before and after the topographic correction. Mean values on the sunny slopes are expected to decrease while those on the shady side are expected to increase for a successful topographic correction.

Tables 1, 2 and 3 show that the cosine correction gives the worst result. There are significant decreases of the mean values together with large increases in the standard deviations in the entire image, herbaceous area and forest area of this image when compared to the original. From table 4, we can also see that the image is overcorrected as the mean values on the shady side become much higher than that on the sunny side. This supports and confirms the general observation of overcorrection of previous researchers e.g. Jones *et al.* 1988.

Surprisingly, the Minnaert corrected image, which gives the best appearance in visual effect, shows a decrease in the mean values and increase in the standard deviations among the three classes in bands 1, 2 and 3. But the extent is relatively small when compared to the cosine corrected image. However, band 4, shows a decrease in the standard deviations for all three classes. Moreover, from table 4, the mean DN values on sunny and shady slopes are similar after the corrections. As a result, this minnaert correction can also be defined as a successful correction.

The normalization method preserved the mean values of the entire image and reduced the values of standard deviations. In the herbaceous area, the mean values decreased slightly and the standard deviations decreased in all the bands. In the forest area, the mean values increased in all four bands and the standard deviations decreased. The decrease of standard deviation is a clearer test of accuracy of each class. In table 4, it also supports the finding, the differences of mean values on sunny slopes and shady slopes reduced after the correction.

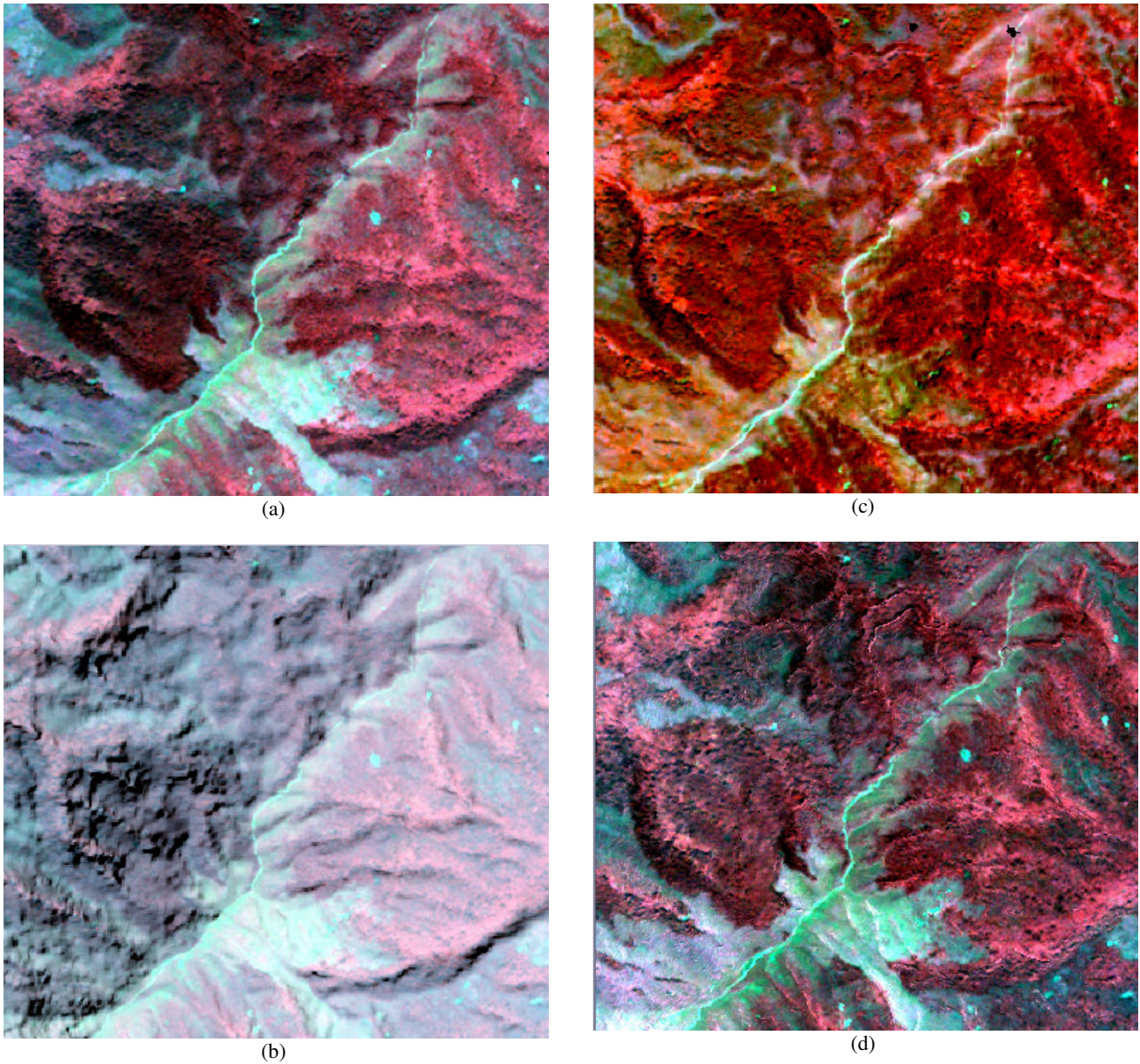


Figure 1. IKONOS False Colour Image, 7 Sept 2002, a ridge from top right to bottom left with sunlight coming from the bottom right, Lam Tseun Country Park. (a) Original image. (b) Result of cosine correction. (c) Result of Minnaert correction. (d) Result of 2-stage normalization

Band	Original Image		Cosine Correction		Minnaert Correction		Normalization	
	μ	σ	μ	σ	μ	σ	μ	σ
1	382.72	36.2	322.08	51.1	364.14	50.3	382.61	35.2
2	398.35	56.0	335.81	66.4	374.16	69.9	397.85	53.0
3	255.47	65.7	215.98	66.0	248.21	71.3	254.76	62.7
4	719.49	111.8	606.51	125.8	727.21	111.1	716.62	109.2

Table 1. Means and standard deviations for the entire study area

	Original Image		Cosine Correction		Minnaert Correction		Normalization	
Band	μ	σ	μ	σ	μ	σ	μ	σ
1	380.54	4.5	333.85	19.3	350.91	14.3	378.22	3.6
2	416.11	12.7	365.25	25.8	379.60	16.1	409.39	10.1
3	261.22	9.4	229.33	17.1	244.16	9.5	255.61	7.8
4	780.71	46.1	685.78	63.6	753.34	41.5	738.83	44.6

Table 2. Means and standard deviations for the herbaceous area

	Original Image		Cosine Correction		Minnaert Correction		Normalization	
Band	μ	σ	μ	σ	μ	σ	μ	σ
1	353.34	7.3	261.82	65.9	311.71	22.1	356.29	6.4
2	347.95	15.2	258.79	68.7	298.12	24.9	355.33	12.1
3	205.13	12.0	152.89	41.9	188.04	13.7	210.80	9.7
4	672.78	91.0	508.03	167.3	671.55	65.1	713.45	67.3

Table 3. Means and standard deviations for the forest area

μ = mean value

σ = standard deviation

Category	Mean Value	Original	cosine correction	Minnaert Correction	Normalization
All	Slope facing to the Sun	748.647	666.066	718.385	702.492
	Slope facing away from the Sun	695.204	556.683	734.652	728.385
Herbaceous	Slope facing to the Sun	787.752	705.725	753.319	732.255
	Slope facing away from the Sun	723.084	569.601	752.369	776.873
Forest	Slope facing to the Sun	765.341	668.833	680.256	709.127
	Slope facing away from the Sun	609.599	400.622	666.191	716.263

Table 4. Mean value of different cover types on different side of slopes of band 4 IKONOS image

5. CONCLUSIONS

Based on the experiments of this study, we have the following conclusions on the three topographic correction methods performed on the IKONOS imagery:

1. The cosine correction is not a suitable method for topographic correction of IKONOS imagery due to the overcorrection.
2. The Minnaert Correction gives the best result visually.
3. The normalization method gives the best result for training areas statistics among the three topographic corrections. This would probably help in improving the result of classification, and further studies will be carried out.
4. A successful topographic correction should preserve the original mean value and decrease in standard deviation.
5. More tests will take to evaluate the effectiveness of topographic correction, e.g. classification result

Further studies would be focus on how the quality of the DEM affects the result of topographic correction of IKONOS imagery.

References

- Civco, D. L., 1989, Topographic Normalization of Landsat Thematic Mapper Digital Imagery, *Photogrammetric Engineering and Remote Sensing*, 55(9), pp. 1303-1309.
- Dakowicz, M. and Gold, C., 2003, Extracting Meaningful Slopes from Terrain Contours, *International Journal of Computational Geometry & Applications*, 13(4), pp.339-357.
- Di, K., Ma, R. and Li, R. X., 2003, Rational Functions and Potential for Rigorous Sensor Model Recovery, *Photogrammetric Engineering and Remote Sensing*, 69(1), pp. 33-41.
- Ekstrand, S., 1996, Landsat TM-Based Forest Damage Assessment: Correction for Topographic Effects, *Photogrammetric Engineering and Remote Sensing*, 62(2), pp. 151-161.

Ferrier, G., 1995, Evaluation of apparent surface reflectance estimation methodologies, *International Journal of Remote Sensing*, 16(12), pp. 2291-2297.

Ganas, A., Lagios, E., and Tzannetos, N., 2002, An investigation into the spatial accuracy of the IKONOS 2 orthoimagery within an urban environment, *International Journal of Remote Sensing*, 23(17), pp. 3513-3519.

Hale, S. R. and Rock, B. N., 2003, Impact of Topographic Normalization on Land-Cover Classification Accuracy, *Photogrammetric Engineering and Remote Sensing*, 69(7), pp. 785-791.

Hanley, H. B. and Fraser, C. S., 2001, Geopositioning accuracy of IKONOS imagery: indications from two dimensional transformations, *Photogrammetric Record*, 17(98), pp. 317-329.

Holben B.N. and Justice C.O., 1980, The Topographic Effect on Spectral Response from Nadir-Pointing Sensors, *Photogrammetric Engineering and Remote Sensing*, 46(9), pp. 1191-1200.

Karpouzli & Malthus, T., 2001, The empirical line method for the atmospheric correction of IKONOS imagery, *Remote Sensing and Photogrammetry Society 2001 Proceedings*.

Itten, K. I. & Meyer, P., 1993, Geometric and Radiometric Correction of TM Data of Mountainous Forested Areas, *Geoscience and Remote Sensing*, 31(4), July.

Mather, P. M., 1999, *Computer processing of remotely sensed images : an introduction*, John Wiley, NY, pp. 94.

Meyer, P., Itten, K., Kellenberger, T., Sandmeier, S. and Sandmeier, R., 1993, Radiometric corrections of topographically induced effects on Landsat TM data in an alpine environment, *ISPRS Journal of Photogrammetry and Remote Sensing*, 48(4), pp. 17-28.

Riaño, D., Chuvieco, E., Salas, J. and Aguado, I., 2003, Assessment of Different Topographic Corrections in Landsat-TM Data for Mapping Vegetation Types, *Geoscience and Remote Sensing*, 41(5), pp. 1056-1061.

Smith, J. A., Lin, T. L. and Ranson, K. J., 1980, The Lambertian Assumption and Landsat Data, *Photogrammetric Engineering and Remote Sensing*, 46(9), pp. 1183-1189

Smith, G. M. and Milton, E.J., 1999, The use of empirical line method to calibrate remotely sensed data to reflectance, *International Journal of Remote Sensing*, 20(13), pp. 2653-2662

Toutin, T. and Cheng, P., 2000, Demystification of IKONOS, *Earth Observation Magazine*, 9(7), pp. 17-21.

Toutin, T., 2003, Error Tracking in Ikonos Geometric Processing Using a 3D Parametric Model, *Photogrammetric Engineering and Remote Sensing*, 69(1), pp. 43-51.

Teillet, P.M., Guindon, B. and Goodenough, D.G., 1982, On the slope-aspect correction of multispectral scanner data, *Canadian Journal of Remote Sensing*, 8(2), pp. 1537-1540.